Macromolecules

Article

pubs.acs.org/Macromolecules

Micellization Properties of Θ-Shaped, Figure-Eight-Shaped and Linked Rings Copolymers

Andreas Kalogirou,[†] Othonas A. Moultos,[§] Leonidas N. Gergidis,[‡] and Costas Vlahos*[,†]

[†]Department of Chemistry, University of Ioannina, 45110 Ioannina, Greece

[‡]Department of Materials Science & Engineering, University of Ioannina, 45110 Ioannina, Greece

[§]Chemical Engineering Program, Texas A&M University at Qatar, P.O. Box 23874, Doha, Qatar

ABSTRACT: The micellization behavior of Θ-shaped, figure-eight-shaped, and linked rings copolymers is studied by means of molecular dynamics simulations with Langevin thermostat. The properties of interest were the critical micelle concentration, the mean aggregation number and the shape of the micelle. We found that the Θ-shaped copolymers form micelles with preferential aggregation numbers. The shape of these micelles is spherical with elongated spherical cores. The homo figure-eight-shaped copolymers also form spherical micelles with preferential aggregation numbers and elongated spherical cores. The mikto figure-eight-shaped and the linked rings copolymers form wormlike or superstructured micelles with a wide range of aggregation numbers. Our simulation results on cmc and the micelles mass distribution are compared with existing experimental findings for the homo and mikto figure-eight-shaped copolymers.

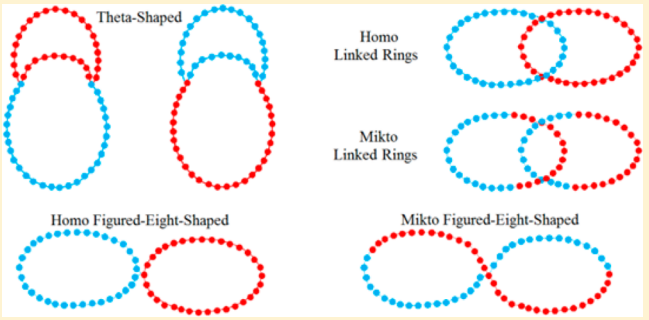

1. INTRODUCTION

The absence of end-groups in ring copolymers leads to significantly different physical properties compared to the linear or branched counterparts both in dilute solution and bulk.[1−5] In dilute solution for the macroscopic state of common Θ solvent the dimensions of ring copolymers are 0.58 times smaller than the respective dimensions of their linear precursors.[2] Experiments[3] of polystyrene-*block*-polyisoprene (PS_{290}-*b*-PI_{110}) diblock copolymers in heptane (a selective solvent for PI) have shown that the cyclization strongly affects the micellization behavior. In every copolymer concentration—up to 20 mg/mL—the linear diblock chains form spherical micelles with diameter of 40 nm with PS core and PI shell. The corresponding cyclic copolymer yields either smaller sun-flower micelles (33 nm in diameter) at very low concentrations, or giant wormlike micelles (up to 1 μm in length) at relative high concentrations. The mechanism for the formation of the latter worm-like structures is the unidirectional self-assembly of the sun flower micelles.[3] Moreover, the thermal stability of sunflower micelles was shown to be increased for more than 40 °C, through the topological conversion of the linear copolymer component, due to the entropic advantage of the cyclic topology.[5]

The considerable progress in polymer synthesis allowed the preparation of complex copolymers, using ring polymers as building blocks. Among these new novel architectures are the double cyclic topologies: Θ-shaped, figure-eight-shaped, and linked rings copolymers (Figure 1, panels a−f). The most general approach for the synthesis of double cyclic copolymers is the intramolecular cyclization of multifunctional precursors bearing two series of complementary functional groups through click reaction under high dilution.[6] For the preparation of Θ-shaped copolymers a three arm A_2B miktoarm star copolymer precursor composed of one polycaprolactone (PCL) and two polystyrene (PS) branches was used.[6] The PCL branch was terminated with two alkylene groups, and the two PS arms had an azide group at the one end.

The figure-eight-shaped copolymers were obtained with the same synthetic strategy, using A_2B_2 miktoarm star precursors that could be classified into two types (Figure 1, panels c and d): homo figure-eight-shaped, when the terminal units of the same kind of arms are connected through click reaction, and mikto figure-eight-shaped, when heteroarm end units are connected.[7−9] The micellization properties of mikto figure-eight-shaped copolymer, which was composed of two AB diblock copolymer rings connected with one unit, were studied and compared to the respective properties of the miktoarm star precursor in selective solvents.[8,9] TEM images[8] have shown that both copolymers self-assembled into spherical micelles. However, there were significant differences in the micelles size. The micelles formed by mikto figure-eight-shaped chains were much bigger, with very large and loose core due to the stretching of the solvophobic blocks.[8] Other TEM images[9] obtained by other researchers, have shown that homo figure-eight-shaped copolymers form micelles of wormlike shape.

Received: May 21, 2014
Revised: July 24, 2014
Published: August 4, 2014

   dx.doi.org/10.1021/ma501053d | *Macromolecules* 2014, 47, 5851−5859

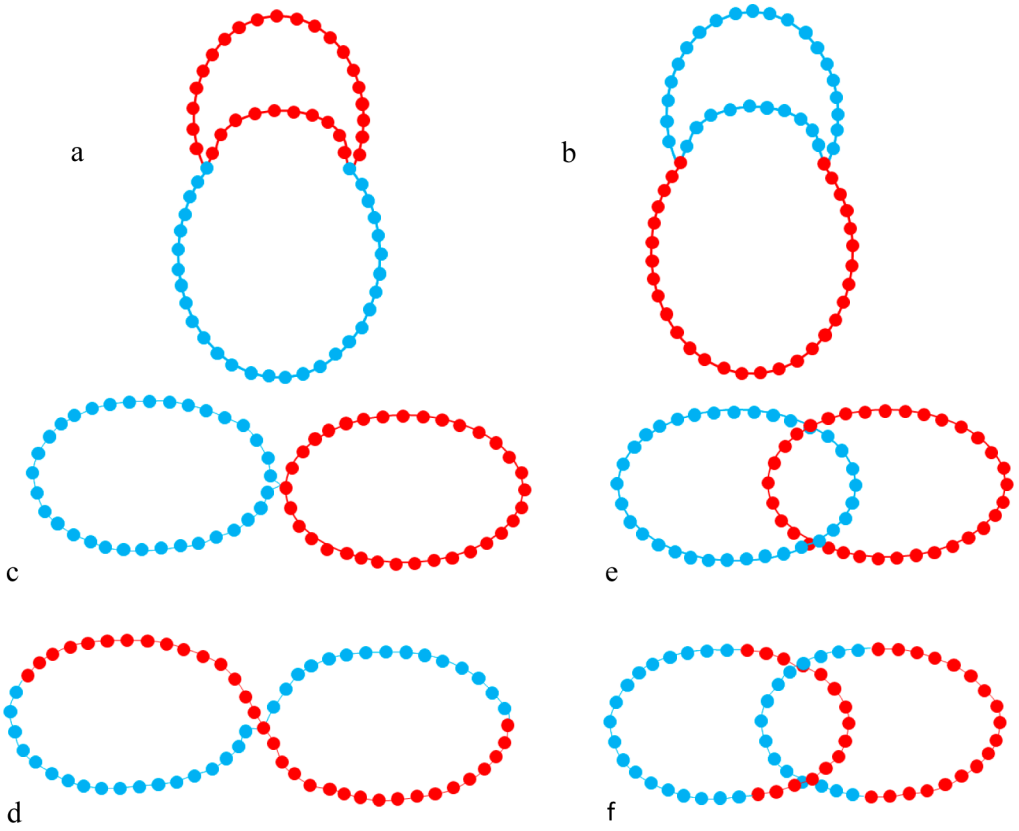

Figure 1. Cartoon representation of (a) Θ-shaped $A_{30}B_{10}B_{20}$, (b) Θ-shaped $A_{10}A_{20}B_{30}$ (c) homo figure-eight-shaped $A_{30}B_{30}$, (d) mikto figure-eight-shaped $A_{30}B_{30}$, (e) homo-linked rings $A_{30}B_{30}$, (f) mikto-linked rings $A_{30}B_{30}$. B units (red) are considered solvophobic and A units (blue) solvophilic.

Recently, polymeric micelles are used as hydrophobic drug carriers.[10] The size, the quantity and the microdynamics of cargo molecules release depend on the size and the porosity of the hydrophobic core. Micelles formed by linear or dendritic blocks are usually considered for that kind of applications.[10,11] In both cases the differences in the porosity of the core are limited.[12] In contrast, with the multiple mixed ring copolymer architectures we are capable of controlling the characteristics of the micelle core by changing the molecular weight of solvophilic and solvophobic blocks in the mixed ring. The solvophilic part of the ring has the tendency to expand the solvophobic counterpart reducing this way core's density. The type of connection of mixed rings is inherently related with the architecture of the copolymer chain (Figure 1). This connection plays an important role in the packing of solvophobic blocks belonging to different rings, influencing the density of the core. Thus, dual ring copolymer architectures could be promising candidates for controlled drug carrier applications taking advantage of their enhanced cargo load and facile release.

We employed molecular dynamics simulations, with Langevin thermostat, in order to elucidate the effect of the dual ring copolymer architecture on the micellization properties. In particular, we studied Θ-shaped copolymers where the two building rings have common subchain (Figure 1, panels a and b), homo and mikto figure-eight-shaped copolymers (Figure 1, panels c and d) where the building rings have a common unit and homo- and mikto-linked rings copolymers (Figure 1, panels e and f) where the building rings interpenetrate each other without common parts. The calculated properties of interest are the critical micelle concentration, the mean aggregation number, the shape and size of the micelle, which is expressed by the shape anisotropy κ^2 and mean squared radius of gyration $\langle R_g^2 \rangle_{micelle}$ respectively.

2. MODEL

In this study, we employed a coarse-grained model to represent the amphiphilic copolymer chains. A group of atoms was modeled as a bead (with diameter σ), while different beads were connected with finitely extensible nonlinear elastic bonds (FENE). A key physical characteristic of polymer molecules is that the chains cannot cross. The FENE potential inherently achieves this, being harmonic at its minimum, while the bonds cannot be stretched beyond a maximum length determined by R_0.The FENE potential is expressed as

$$U_{Bond}(r_{ij}) = \begin{cases} -0.5kR_0^2 \ln\left[1 - \left(\frac{r_{ij}}{R_0}\right)^2\right], & r_{ij} \le R_0 \\ \infty, & r_{ij} > R_0 \end{cases} \quad (1)$$

where r_{ij} is the distance between beads i and j, $k = 25T\varepsilon/\sigma^2$ and R_0 is the maximum extension of the bond ($R_0 = 1.5\sigma$). These parameters[13,14] prevent chain crossing by ensuring an average bond length of 0.97σ. Monomer−monomer interactions were calculated by means of a truncated and shifted Lennard-Jones potential:

dx.doi.org/10.1021/ma501053d | Macromolecules 2014, 47, 5851−5859

$$U_{LJ}(r_{ij}) = \begin{cases} 4\varepsilon_{ij}\left[\left(\frac{\sigma}{r_{ij}}\right)^{12} - \left(\frac{\sigma}{r_{ij}}\right)^{6} - \left(\frac{\sigma}{r_{cij}}\right)^{12} + \left(\frac{\sigma}{r_{cij}}\right)^{6}\right] + \varepsilon_{ij}, & r_{ij} \le r_{cij} \\ 0, & r_{ij} > r_{cij} \end{cases} \tag{2}$$

where ε_{ij} is the well-depth, and r_{cij} is the cutoff radius. The solvent molecules are considered implicitly. The short time-steps needed to model solvent's behavior (the fast motion) restrict the time scales that maybe sampled, thereby limiting the information that can be obtained for the slower motion of the copolymer. Molecular dynamics simulation with Langevin thermostat allows the statistical treatment of the solvent, incorporating its influence on the copolymer by a combination of random forces and frictional terms. The friction coefficient and the random force couple the simulated system to a heat bath and therefore the simulation has canonical ensemble (NVT) constraints. The equation of motion of each bead i of mass m in the simulation box follows the Langevin equation:

$$m_i\ddot{\mathbf{r}}_i(t) = -\nabla \sum_j \left[U_{LJ}(r_{ij}) + U_{Bond}(r_{ij})\right] - m_i\xi\dot{\mathbf{r}}_i(t) + \mathbf{F}_i(t) \tag{3}$$

where m_i, $\mathbf{r}_i$, and ξ are the mass, the position vector, and the friction coefficient of the i bead, respectively. The friction coefficient is equal to $\xi = 0.5\tau^{-1}$, with $\tau = \sigma\sqrt{m/\varepsilon}$. The random force vector $\boldsymbol{F}_i$ is assumed to be Gaussian, with zero mean, and satisfies the equation

$$\langle \mathbf{F}_i(t)\cdot\mathbf{F}_j(t')\rangle = 6k_B T m\xi\delta_{ij}\delta(t - t') \tag{4}$$

k_B is the Boltzmann constant and T is the temperature.

In amphiphilic copolymers studied here, A beads are considered solvophilic and B beads solvophobic. In every conducted simulation the solvophobic part B of the copolymer contained 30 beads, while the length of the A part was varied consisted of 16, 30, and 60 units. In the case of Θ-shaped copolymers, the solvophilic units are distributed to one or two of the three subchains denoted as $A_8A_8B_{30}$, $A_4A_{12}B_{30}$, $A_{16}B_{10}B_{20}$, $A_{15}A_{15}B_{30}$, $A_{10}A_{20}B_{30}$, $A_{30}B_{10}B_{20}$, $A_{30}A_{30}B_{30}$, $A_{20}A_{40}B_{30}$, and $A_{60}B_{10}B_{20}$. In the case of homo figure-eight-shaped and homo linked rings copolymers, the solvophilic units are distributed in one of the two rings denoted as $A_{16}B_{30}$, $A_{30}B_{30}$, and $A_{60}B_{30}$, while in mikto figure-eight-shaped and mikto linked rings copolymers both rings are diblock copolymers $(A_8B_{15})_2$, $(A_{15}B_{15})_2$, and $(A_{30}B_{15})_2$.

Molecular dynamics simulations with Langevin thermostat were performed in a cubic box with periodic boundary conditions, using the open-source massive parallel simulator LAMMPS.[15] Various earlier studies have proved the high efficiency of LAMMPS in the study of amphiphilic copolymers.[14,16,17] The reduced temperature of the simulation T^* was set to $T^*=k_BT/\varepsilon = 1.8$. This choice of temperature allows the studied systems to have both micelles and free molecules.[14] If the temperature is very low, the studied system contains only aggregates and no free molecules; while if the temperature is very high, the studied system contains only free molecules and no aggregates. Different cutoff distances in the Lennard-Jones potential were used[14,16−18] to describe the interactions between copolymer units. The A−A and A−B interactions were considered repulsive and have cutoff radii $r_{cij}=2^{1/6}\sigma$. This cutoff radius is very efficient to reproduce the critical exponent value of the radius of gyration of polymers in the athermal regime for the range of molecular weights used in this work. To introduce the effect of poor solvent for the B units we extend the range of interactions to $r_{cij} = 2.5\sigma$. The potential is practically zero at the cutoff distance introducing an error around $\varepsilon/60 = 1.6\%$. However, in order to study the net effect of architecture on micellization properties of copolymers we used the same cutoff radii, molecular weight of solvophobic units and the same reduced temperature $T^* = 1.8$. For the sake of simplicity, all types of beads were considered to have the same mass ($m = 1$) and diameter ($\sigma = 1$). Copolymers were assumed to reside to the same micelle if the distance between any two nonbonded solvophobic beads B, belonging to different chains, was found within 1.5σ. The aforementioned criterion has been adopted by the literature for the description of the micellization process where this distance corresponds to the maximum extension of the FENE bonds.[13] In all simulations, we set $\varepsilon = 1$.

In the current study, systems containing 125 copolymer chains were simulated for the calculation of the cmc values. All other properties were computed from systems with 1000 chains at total copolymer concentration [C] = 0.12 where most aggregates are formed.[14] The system size was chosen so to prevent the largest micelles from having a radius of gyration greater than the one-fourth of the box side length. The use of the one-quarter of the simulation box side proved to be a sufficient condition to avoid interaction of chains and micelles with their images. No system size effects were observed for all the calculated quantities reported in this paper.

In order to avoid bond crossing at the desired concentration, copolymer chains were initially arranged on a lattice box. The energy of the chains was minimized and then the lattice box was replicated in order to obtain the desired number of chains. We performed 1 million time steps with integration step $\Delta t = 0.008\tau$ setting all cutoff radii equal to $r_{cij} = 2^{1/6}\sigma$ in order to eliminate any bias introduced from the initial conformation. Then, the system was allowed to equilibrate for 10 million steps. The simulation was subsequently conducted for 10 million steps for the systems with 125 copolymer chains, and 60 million steps for the larger systems with 1000 amphiphiles. The duration of the simulation was evaluated by calculating the tracer autocorrelation function:

$$C(t) = \frac{\langle N(t_0 + t)N(t_0)\rangle - \langle N(t_0)\rangle^2}{\langle N^2(t_0)\rangle - \langle N(t_0)\rangle^2} \tag{5}$$

where $N(t)$ is the number of molecules in the micelle in which the copolymer resides at time t. We took all copolymers as tracers, and every time step as a time origin t_0. The characteristic relaxation time t_{relax} is defined as the required time for $C(t)$ to reach the value[14] of e^{-1}. Each simulation was conducted for at least $10t_{relax}$ in order to have 10 independent conformations. The properties of interest were calculated as averages from 1000 and 2000 snapshots for the systems with 125 and 1000 chains, respectively.

3. RESULTS AND DISCUSSION

3.1. Critical Micelle Concentration. Critical micelle concentration (cmc) is an important property of self-assembly because it is a direct measure of the thermodynamic stability of the micelles in the solution. In general, amphiphilic copolymers with lower cmc values are stable at lower concentration. The onset of micellization is traditionally depicted by plotting the free (nonassociated) copolymer monomers concentration [F] as a function of the total copolymer monomers concentration

dx.doi.org/10.1021/ma501053d | Macromolecules 2014, 47, 5851−5859

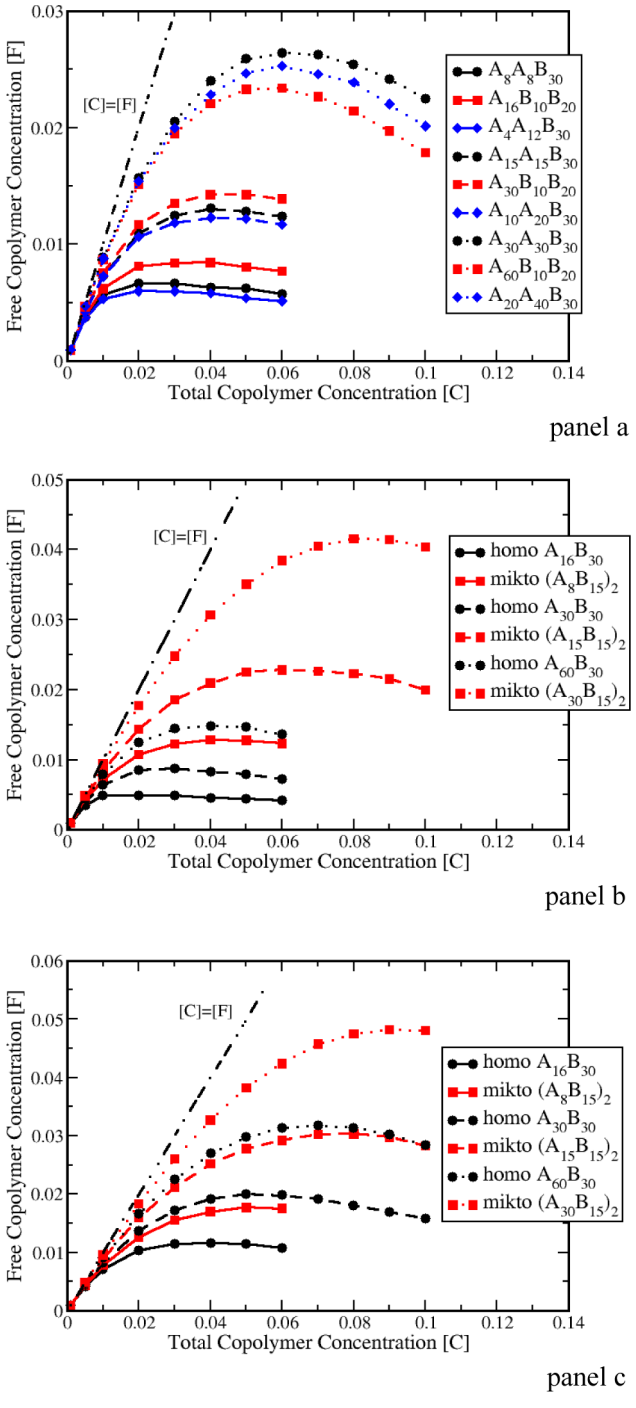

Figure 2. Concentration of the free copolymers [F] versus the total copolymer concentration [C] for Θ-shaped (panel a), figure-eight-shaped (panel b), and linked rings copolymers (panel c).

[C]. For ideal systems as [C] increases small micelles are formed and the concentration of free chains reduces progressively reaching a plateau at the cmc. For higher copolymer concentration [C], the nonidealities introduced by the excluded volume interactions reduce the free chain concentration and the maximum value of [C] defines the cmc for real systems.[14] More or less, at the cmc, 5% of the mole fraction of amphiphilic copolymers are contained in micelles.[19] Figure 2 shows plots of the total free copolymer concentration [F] against the total copolymer concentration [C] for the simulated Θ-shaped, figure-eight-shaped, and linked rings

Table 1. Values of cmc for Different Θ-Shaped, Figure-Eight-Shaped, and Linked Rings Copolymers

	M_w	solvophobic content (%)	cmc	r
		Θ-Shaped		
$A_8A_8B_{30}$	46	65.2	0.0067	1.875
$A_{16}B_{10}B_{20}$	46	65.2	0.0085	1.875
$A_4A_{12}B_{30}$	46	65.2	0.006	1.875
$A_{15}A_{15}B_{30}$	60	50	0.013	1
$A_{30}B_{10}B_{20}$	60	50	0.014	1
$A_{10}A_{20}B_{30}$	60	50	0.012	1
$A_{30}A_{30}B_{30}$	90	33.3	0.026	0.5
$A_{60}B_{10}B_{20}$	90	33.3	0.023	0.5
$A_{20}A_{40}B_{30}$	90	33.3	0.025	0.5
		Figure-Eight-Shaped		
homo $A_{16}B_{30}$	46	65.2	0.005	1.875
mikto $(A_8B_{15})_2$	46	65.2	0.013	1.875
homo $A_{30}B_{30}$	60	50	0.0088	1
mikto $(A_{15}B_{15})_2$	60	50	0.023	1
homo $A_{60}B_{30}$	90	33.3	0.015	0.5
mikto $(A_{30}B_{15})_2$	90	33.3	0.042	0.5
		Linked Rings		
homo $A_{16}B_{30}$	46	65.2	0.012	1.875
mikto $(A_8B_{15})_2$	46	65.2	0.018	1.875
homo $A_{30}B_{30}$	60	50	0.02	1
mikto $(A_{15}B_{15})_2$	60	50	0.03	1
homo $A_{60}B_{30}$	90	33.3	0.032	0.5
mikto $(A_{30}B_{15})_2$	90	33.3	0.048	0.5

amphiphilic copolymers. The cmc values calculated from Figure 2 are given in Table 1. The molecular theory for the formation of micelles can be used to describe qualitatively the trends of these values.[20] According to the theory the driving force of aggregation is the change in the Gibbs free energy g_{mic} associated with the transfer of n unimers from the solution to a micelle. The higher the g_{mic} the higher the cmc value. For uncharged copolymers g_{mic} can be modeled as the sum of four different terms that takes into account all of the free energy changes that occur upon micelle formation[19] $g_{mic} = g_{tr} + g_{int} + g_{pack} + g_{st}$. The first three terms are related to the solvophobic part of the copolymer, and the fourth is associated with the solvophilic counterpart. The free energy of transfer g_{tr} reflects the energy change associated with the transfer of the solvophobic block from the solution to micelles core. The interfacial free energy g_{int} takes into account the energy change upon the formation of the interface between the core and the solution while g_{pack} involves the free energy change associated with the packing of the solvophobic part into the micelle core. The last term g_{st} accounts for the contribution of steric interactions between the solvophilic units of the copolymers.

Table 1 shows that for symmetric $A_{N1}A_{N2}B_{30}$ Θ-shaped copolymers (with equal length solvophilic subchains $N_1 = N_2$), the cmc values are proportional to the subchain length. The larger the solvophilic subchains become the higher the steric penalties for transferring the large groups into the micelle. According to the analytical theory of micellization g_{mic} increases and consequently cmc values increase. For similar reasons the cmc of asymmetric Θ-shaped copolymers $A_4A_{12}B_{30}$, $A_{10}A_{20}B_{30}$, and $A_{20}A_{40}B_{30}$ increases almost linearly as the solvophilic subchains length increases. Between the Θ-shaped copolymers with two solvophilic subchains, having the same total molecular weight and solvophobic/solvophilic units ratio r, the copolymer having the higher cmc values is the one with with the

dx.doi.org/10.1021/ma501053d | Macromolecules 2014, 47, 5851−5859

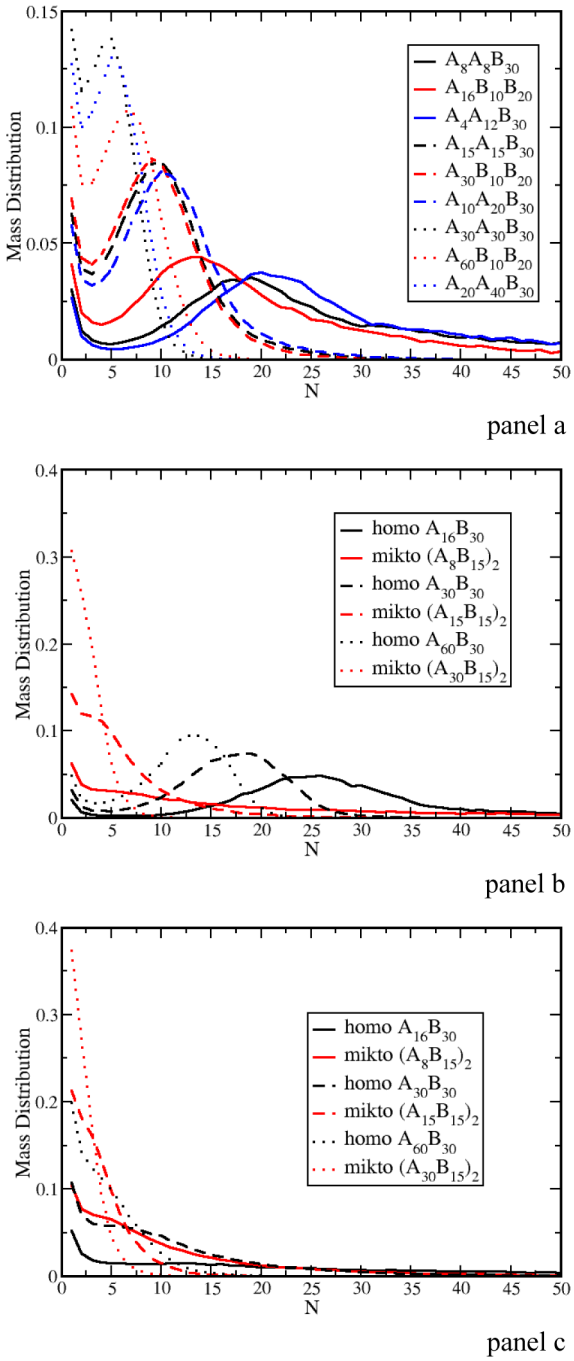

Figure 3. Mass distribution of the aggregates for Θ-shaped (panel a), figure-eight-shaped (panel b), and linked rings copolymers (panel c).

symmetric subchains. This is due to the higher steric interactions between the subchains in the corona. The cmc values of Θ-shaped copolymers containing two solvophobic subchains also exhibit a monotonic increase as the solvophobic content decreases. For small (M_w = 46) and moderate (M_w = 60) total molecular weights the cmc values of $A_{16}B_{10}B_{20}$ and $A_{30}B_{10}B_{20}$ Θ-shaped copolymers with two solvophobic subchains are higher than the respective cmc values of asymmetric and symmetric $A_4A_{12}B_{30}$, $A_8A_8B_{30}$, $A_{10}A_{20}B_{30}$, and $A_{15}A_{15}B_{30}$ copolymers with two solvophilic subchains having the same M_w and ratio r. The reason for this is the different interfacial energy per chain g_{int} needed from these copolymers in the process of aggregation. In the case of the copolymers, $A_4A_{12}B_{30}$ and $A_8A_8B_{30}$, the long solvophobic subchain could extend far away from the two connection points with the solvophilic subchain, thus reducing the interface with the solvent and consequently the enthalpic interactions with the solvent. Moreover, the extension of the large subchain increases the interface exposed to other copolymers' solvophobic moieties, resulting in a higher probability of interaction with them and, furthermore, reducing the free energy of the copolymers. For larger molecular weights (M_w = 90) the trends are reversed and the cmc values of $A_{60}B_{10}B_{20}$ are lower than the values of $A_{15}A_{15}B_{30}$ and $A_{20}A_{40}B_{30}$ copolymers. In order to clarify these results we have calculated the root of mean square distance between the subchains common ends $\langle R^2\rangle^{1/2}$. For the $A_8A_8B_{30}$, $A_{15}A_{15}B_{30}$, $A_{30}A_{30}B_{30}$, $A_{16}B_{10}B_{20}$, $A_{30}B_{10}B_{20}$, and $A_{60}B_{10}B_{20}$, we found that the $\langle R^2\rangle^{1/2}$ distance of Θ copolymers associated in micelles is equal to 3.15, 3.75, 4.45, 2.97, 3.13, and 3.21 respectively. The same property for the free Θ-shaped copolymer chains in the solution attains the values of 3.22, 3.83, 4.59, 2.99, 3.14, and 3.21. As expected, the difference in $\langle R^2\rangle^{1/2}$ value between the free and the associated copolymer chain is negligible in all cases. However, the $\langle R^2\rangle^{1/2}$ value, for $A_{30}A_{30}B_{30}$ copolymer is about 40% larger than the respective value of $A_8A_8B_{30}$. In the case of $A_{16}B_{10}B_{20}$ and $A_{60}B_{10}B_{20}$ copolymers the difference in $\langle R^2\rangle^{1/2}$ is around 8%. This indicates that the increase in the length of two solvophilic subchains enforces the solvophobic part to have larger size, increasing the interface with the solvent and consequently the cmc.

In the case of homo figure-eight-shaped copolymers the two homopolymeric rings have only one common junction. This way the shrinkage of solvophobic ring in the selective solvent is not influenced by the presence of the solvophilic counterpart, as in the case of Θ-shaped copolymer where the two rings have a common arc (subchain) either solvophilic or solvophobic. Therefore, the cmc values presented in Table 1 are always lower than the respective values of both types of Θ-shaped copolymers. As the molecular weight of solvophilic ring increases from $A_{16}B_{30}$, to $A_{30}B_{30}$ and $A_{60}B_{30}$ the cmc values increase monotonously following the general rule: the lower the solvophobic/solvophilic units ratio r the higher the cmc. In contrast, the mikto figure-eight-shaped copolymers have higher cmc values than the respective Θ-shaped copolymers. The reason is 2-fold. In mikto figure-eight-shaped copolymers $(A_8B_{15})_2$ there are two A_8 subchains forming the corona, instead of one A_{16} as in Θ-shaped $A_{16}B_{10}B_{20}$, and consequently higher steric interactions are introduced. Moreover, the two B_{15} subchains residing in the core of the micelle have three junction points (instead of two $B_{10}B_{20}$ Θ-shaped) that should be placed in the periphery of the core leading to larger interfacial energy g_{int}.

In Table 1, we also present the cmc results for the linked rings copolymers. The homo-linked rings consists of two linked homopolymeric rings while in the mikto-linked rings two identical diblock copolymeric rings are linked. It can be observed that the cmc values of the homo-linked rings are two times higher than the cmc values of the homo figure-eight-shaped copolymers, with the same ratio r and total molecular weight, and very close to the respective mikto figure-eight-shaped copolymers. The reason is that a considerable part of solvophobic units (which entangle with solvophilic ring) is enforced to reside out of the solvophobic core, being that way in direct contact with the solvent consequently having high interfacial energy. The highest cmc values of all architectures

dx.doi.org/10.1021/ma501053d | Macromolecules 2014, 47, 5851−5859

Table 2. Shape Characteristics of the Most Probable Aggregates Formed by Θ-Shaped, Figure-Eight-Shaped, and Linked Rings Copolymers

	N_p	$\langle R_g^2\rangle_{micelle}$	$\langle R_g^2\rangle_{core}$	$\langle R_g^2\rangle_{corona}$	$\langle \kappa^2\rangle_{micelle}$	$\langle \kappa^2\rangle_{core}$
			Θ-Shaped			
$A_8A_8B_{30}$	19	46.6 (0.6)	36.3 (0.7)	65.9 (0.5)	0.123 (0.006)	0.183 (0.007)
$A_{16}B_{10}B_{20}$	14	39.4 (0.4)	29.6 (0.4)	57.6 (0.4)	0.133 (0.005)	0.216 (0.005)
$A_4A_{12}B_{30}$	20	46.4 (0.4)	34.8 (0.5)	67.7 (0.4)	0.104 (0.006)	0.164 (0.007)
$A_{15}A_{15}B_{30}$	10	41.7 (0.2)	24.7 (0.2)	58.4 (0.2)	0.092 (0.003)	0.181 (0.004)
$A_{30}B_{10}B_{20}$	9	41.0 (0.2)	20.8 (0.2)	60.7 (0.2)	0.078 (0.001)	0.189 (0.001)
$A_{10}A_{20}B_{30}$	10	41.8 (0.2)	24.0 (0.3)	59.3 (0.2)	0.085 (0.002)	0.173 (0.003)
$A_{30}A_{30}B_{30}$	5	43.93 (0.06)	16.3 (0.1)	57.2 (0.1)	0.0845 (0.0003)	0.195 (0.002)
$A_{60}B_{10}B_{20}$	7	60.5 (0.1)	17.3 (0.1)	81.3 (0.2)	0.0692 (0.0007)	0.187 (0.003)
$A_{20}A_{40}B_{30}$	5	45.63 (0.08)	16.1 (0.1)	59.7 (0.1)	0.0892 (0.0007)	0.193 (0.001)
			Figure-Eight-Shaped			
homo $A_{16}B_{30}$	26	56 (1)	35.7 (0.5)	94 (3)	0.093 (0.006)	0.140 (0.007)
homo $A_{30}B_{30}$	19	65 (1)	28.6 (0.3)	103 (2)	0.064 (0.004)	0.126 (0.005)
homo $A_{60}B_{30}$	13	93 (2)	22.1 (0.1)	127 (2)	0.053 (0.003)	0.120 (0.002)
			Linked Rings			
homo $A_{16}B_{30}$	12	46.4 (0.4)	40.3 (0.4)	57.5 (0.4)	0.180 (0.006)	0.227 (0.008)

studied in the present paper are obtained from the mikto-linked rings copolymers. Snapshots of the micelles show that due to the free rotation of linked copolymer rings, large solvophobic parts are exposed directly to the solvent increasing this way the interfacial energy of the micelle and consequently the cmc.

3.2. Micelle Size and Shape. The aggregation number, the radii of gyration of the solvophobic, solvophilic parts and of the whole aggregate as well as the resulting shape anisotropy κ^2 are useful tools for the characterization of the micelles formed by amphiphilic copolymers. Shape anisotropy is defined as

$$\kappa^2 = 1 - 3\frac{\langle I_2\rangle}{\langle I_1^2\rangle} \quad (6)$$

where I_1 and I_2 are the first and second invariants of the radius of gyration tensor. The value of shape anisotropy $\kappa^2 = 0$ corresponds to perfect sphere while $\kappa^2 = 1$ to perfect rod. All these properties were calculated on the most concentrated system having [C] = 0.12, where most aggregates are formed. Results on the mass distribution of the aggregates for various Θ-shaped, figure-eight-shaped, and linked rings copolymers are shown in Figure 3. In the case of Θ-shaped copolymers (Figure 3, panel a), the mass distribution of the aggregates has a maximum value corresponding to the preferential aggregation number N_p of the formed micelles. The N_p values and the other shape and size characteristics of micelles are presented in Table 2. It can be observed that between copolymers with the same total molecular weight and solvophobic/solvophilic units ratio r, those with smaller cmc form micelles with higher preferential aggregation number N_p. The shape of preferential micelles of $A_4A_{12}B_{30}$ copolymers (N_p = 20, M_w = 46), with two asymmetric solvophilic subchains, is spherical with $\langle\kappa^2\rangle_{micelle}$ = 0.104 while the solvophobic core is elongated sphere with $\langle\kappa^2\rangle_{core}$ = 0.164 (Figure 4a). Micelles with $N_p \geq 35$ have a wormlike shape with $\langle\kappa^2\rangle_{micelle}$ = 0.34 and $\langle\kappa^2\rangle_{core}$ = 0.43 (Table 3). The core radius of gyration of preferential micelles of $A_4A_{12}B_{30}$ is around 15% larger compared to the respective core of micelles formed by asymmetric miktoarm star $(A_2)_2(A_{13})_2B_{30}$ having four solvophilic and one solvophobic arms. The star micelles have the same aggregation number N_p =20 and the same solvophobic units but greater solvophilic content.[17] The $A_8A_8B_{30}$ copolymer with the symmetric solvophilic subchains forms aggregates with similar preferential aggregation number N_p =19 and shape closer to the elongated sphere ($\langle\kappa^2\rangle_{micelle}$ = 0.123, $\langle\kappa^2\rangle_{core}$ = 0.183). Snapshot analysis (Figure 4b) shows that the core having an elongated sphere shape, may contain multiple solvophobic regions. However, the density profile curve plotted along the micelle's core center of mass is smooth indicating a significant overlapping of solvophobic regions (Figure 5).

The third type of Θ-shaped copolymers, those with two solvophobic subchains $A_{16}B_{10}B_{20}$, form smaller preferential aggregates due to the larger interfacial energy as we explained in the previous section. The $\langle\kappa^2\rangle_{micelle}$ is 0.133, a value which is closer to the respective value for the symmetric $A_8A_8B_{30}$ copolymers. In the case of Θ-shaped copolymers with M_w = 60 and r = 1 all preferential micelles have similar aggregation numbers $N_p \approx 10$. The shape of micelles formed by $A_{15}A_{15}B_{30}$ and $A_{30}B_{10}B_{20}$ copolymers is spherical with $\langle\kappa^2\rangle_{micelle}$ = 0.092, 0.078 respectively due to the more spherical corona while the core shape is an elongated sphere with $\langle\kappa^2\rangle_{core}$ = 0.181 and 0.189. The $A_{10}A_{20}B_{30}$ copolymers, with two asymmetric subchains in the corona, form elongated spherical micelles with elongated spherical cores. The $A_{10}A_{20}B_{30}$ aggregates with $N_p \geq 20$ are wormlike in shape. Further increase of the length of the solvophilic subchains (M_w = 90 and r = 0.5) leads to micelles with smaller aggregation numbers. As it can be observed from the values of Table 2 the micelles are spherical with elongated spherical cores. System snapshots revealed that wormlike micelles are not formed, due to the long solvophilic subchains.

The mass distributions of micelles for the homo and mikto figure-eight-shaped copolymers are presented in Figure 3b. It can be observed that all the homo figure-eight-shaped copolymers $A_{16}B_{30}$, $A_{30}B_{30}$, and $A_{60}B_{30}$ form micelles with preferential aggregation numbers N_p = 26, 19, and 13 respectively. These values are less than the half of the aggregation numbers of the respective linear diblock copolymer[14] having N_p = 62, 41, and 38. However, the aforementioned N_p values obtained by the simulations are much smaller than the respective experimental ones since the number of solvophobic units considered in the simulations is very small compared to that of real copolymers. The shape of the preferential micelles is almost spherical (Figure 4c) while $\langle\kappa^2\rangle_{micelle}$ decreases as the solvophilic content increases. However, $A_{16}B_{30}$ micelles with higher $N_p \geq 34$ are wormlike

dx.doi.org/10.1021/ma501053d | Macromolecules 2014, 47, 5851−5859

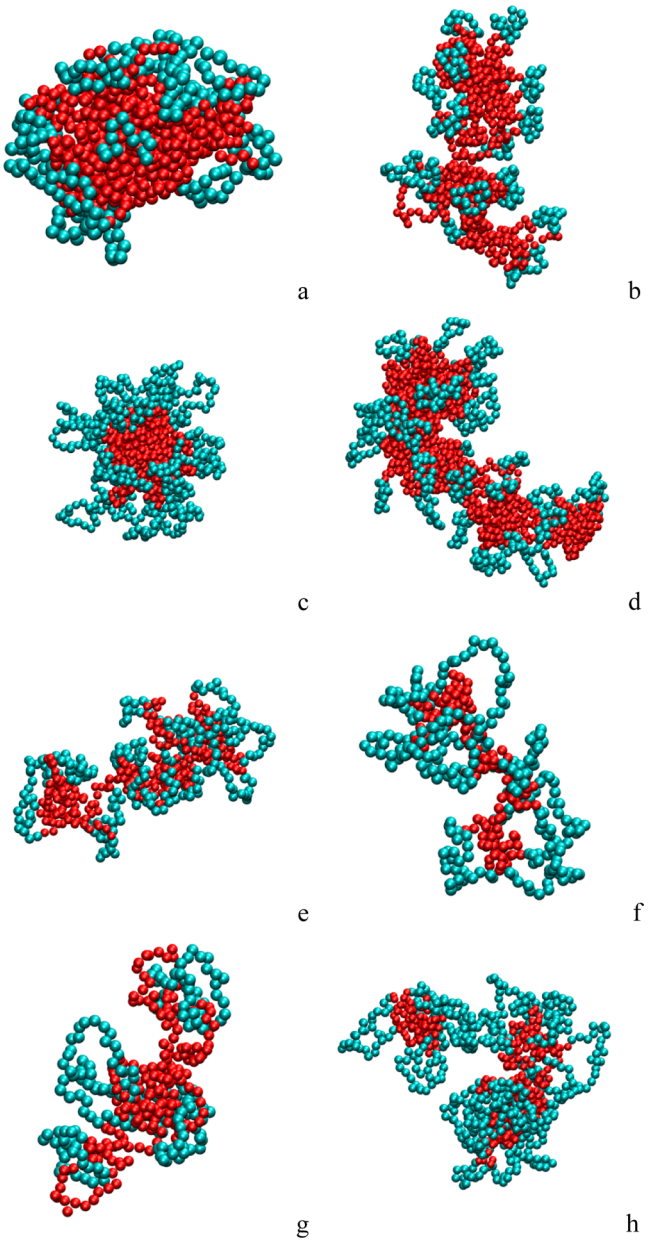

Figure 4. Snapshots of micelles formed by (a) Θ-shaped $A_4A_{12}B_{30}$ N_p =20, (b) Θ-shaped $A_8A_8B_{30}$ N_p =19, (c) homo figure-eight-shaped $A_{30}B_{30}$ N_p = 19, (d) homo figure-eight-shaped $A_{16}B_{30}$ N_p = 34, (e) mikto figure-eight-shaped $(A_{15}B_{15})_2$ N_p = 10, (f) mikto figure-eight-shaped $(A_{30}B_{15})_2$ N_p = 5, (g) homo-linked rings $A_{30}B_{30}$ N_p = 7, (h) mikto-linked rings copolymers $(A_{30}B_{15})_2$ N_p = 10.

with $\langle\kappa^2\rangle_{micelle}$ = 0.15 and $\langle\kappa^2\rangle_{core}$ = 0.23 (Figure 4d). In the case of mikto figure-eight-shaped copolymers, where each one of the two rings is a diblock copolymer, the mass distribution of micelles is not monotonic indicating a wide spectra of aggregation numbers. The solvophobic subchains belonging to individual rings of the copolymer behave as two independent sticky patches leading to the formation of wormlike micelles with wide aggregation numbers (Figure 4e,f).

The results concerning the linked rings copolymers are presented in Figure 3c and at Tables 2 and 3. It can be observed that homo-linked rings copolymers $A_{16}B_{30}$ containing two homopolymeric-linked rings form elongated micelles with preferential aggregation number N_p = 12. All other homo-linked ring copolymers form wormlike micelles with wide aggregation numbers (Figure 4g). The mikto-linked rings copolymers $(A_8B_{15})_2$, $(A_{15}B_{15})_2$, and $(A_{30}B_{15})_2$ also form wormlike micelles with wide aggregation numbers. The characteristic of the wormlike micelles formed by the mikto-linked rings copolymers is the presence of multiple, separated cores, which are connected through solvophilic bridges (Figure 4h). The reason is that the two solvophobic subchains are placed at both ends of copolymer, creating two sticky patches necessary for the wormlike micelle formation.

3.3. Comparison with Experiments. As mentioned in the Introduction the micellization properties of homo and mikto figure-eight-shaped copolymers have been studied experimentally.[8,9] Isono et al.[9] have synthesized figure-eight-shaped copolymers with total $M_n \approx 22\,000$ and solvophobic/solvophilic ratio $r \approx 1$. Both solvophilic and solvophobic monomers had the same length, differing in the side groups. Isono et al.[9] showed that the cmc of homo figure-eight-shaped copolymers is smaller than the cmc of the respective mikto figure-eight-shaped which is in full agreement with our simulation results. Their reported cmc value for homo figure-eight-shaped copolymer was smaller than the value of the respective linear diblock copolymer. This unusual result might be attributed to the larger molecular weight of homo figure-eight-shaped copolymers, since cmc is very sensitive upon the increase of solvophobic's part molecular weight.

Fan et al.[8] studied the micellization properties of mikto figure-eight-shaped copolymers and their four arm miktoarm star copolymer precursors. Although, the authors[8] mention that figure-eight-shaped copolymers form very large spherical micelles with loose core, the TEM images (Figure 6A,B of ref 8) indicate that mikto figure-eight-shaped copolymer micelles may have wormlike shape, composed of two or three smaller spherical micelles connected to each other, similar to our findings depicted in Figure 4e,f. The micelles size distribution, presented in Figure 7A in the same manuscript,[8] also indicates the presence of very large aggregates. The aforementioned sizes are several times larger than their respective miktoarm star precursors which may indicate the formation of wormlike micelles, obtained from the connection of smaller spherical ones.

Results on homo figure-eight-shaped copolymers are reported by Isono et al.[9] The TEM images (Figure S14 VII of ref 9) show that the formed micelles have wormlike shape. Our simulation results, indicate the formation of spherical micelles for preferential aggregation number N_p = 19 and wormlike micelles for much larger N_p. This discrepancy could possibly be explained by the small ring lengths used in our simulations, or by some factors related to the synthetic process such as the formation of knots, which is a known issue in synthesis of ring architectures, both for homopolymers and copolymers.[21,22] Further experimental and theoretical studies are required for the elucidation of the role of multiring architecture on the micellization properties of copolymers.

■ CONCLUSIONS

The micellization behavior of double cyclic copolymers is studied by means of molecular dynamics simulations with Langevin thermostat. In particular, we studied Θ-shaped copolymers with one and two solvophobic subchains, homo and mikto figure-eight-shaped copolymers, where the building rings were homopolymers or symmetric diblock copolymers, and homo- and mikto-linked rings copolymers. The properties

dx.doi.org/10.1021/ma501053d | Macromolecules 2014, 47, 5851−5859

Table 3. Shape Characteristics of Aggregates Formed by Θ-Shaped, Figure-Eight-Shaped, and Linked Rings Copolymers

	N_p	$\langle R_g^2\rangle_{micelle}$	$\langle R_g^2\rangle_{core}$	$\langle R_g^2\rangle_{corona}$	$\langle \kappa^2\rangle_{micelle}$	$\langle \kappa^2\rangle_{core}$
			Θ-Shaped			
$A_4A_{12}B_{30}$	40	114 (3)	101 (3)	136 (3)	0.34 (0.01)	0.43 (0.02)
$A_{10}A_{20}B_{30}$	20	88 (2)	68 (2)	108 (2)	0.26 (0.01)	0.41 (0.02)
$A_{20}A_{40}B_{30}$	10	69.3 (0.5)	31.4 (0.6)	87.9 (0.6)	0.092 (0.003)	0.26 (0.01)
			Figure-Eight-Shaped			
homo $A_{60}B_{30}$	20	112 (5)	30.8 (0.9)	152 (7)	0.05 (0.01)	0.14 (0.01)
homo $A_{30}B_{30}$	26	81 (4)	41 (2)	121 (7)	0.10 (0.01)	0.21 (0.02)
homo $A_{16}B_{30}$	40	92 (6)	71 (6)	131 (6)	0.27 (0.03)	0.39 (0.03)
mikto $(A_8B_{15})_2$	10	45.3 (0.7)	41.0 (0.7)	53.3 (0.7)	0.249 (0.006)	0.300 (0.008)
mikto $(A_8B_{15})_2$	22	104 (2)	99 (2)	113 (2)	0.30 (0.01)	0.33 (0.01)
mikto $(A_{15}B_{15})_2$	5	32.5 (0.2)	23.4 (0.2)	41.3 (0.2)	0.182 (0.002)	0.299 (0.003)
mikto $(A_{15}B_{15})_2$	10	67.4 (0.7)	57.3 (0.7)	77.3 (0.7)	0.282 (0.006)	0.381 (0.007)
mikto $(A_{15}B_{15})_2$	19	134 (3)	123 (3)	144 (3)	0.31 (0.01)	0.36 (0.01)
mikto $(A_{30}B_{15})_2$	3	33.94 (0.04)	14.94 (0.04)	42.85 (0.05)	0.131 (0.001)	0.293 (0.001)
mikto $(A_{30}B_{15})_2$	5	49.9 (0.2)	27.8 (0.2)	60.6 (0.2)	0.151 (0.002)	0.353 (0.003)
			Linked Rings			
homo $A_{16}B_{30}$	35	141 (7)	134 (7)	154 (8)	0.30 (0.02)	0.33 (0.02)
homo $A_{30}B_{30}$	7	43.9 (0.2)	31.0 (0.1)	56.4 (0.2)	0.160 (0.002)	0.253 (0.002)
homo $A_{30}B_{30}$	24	144 (2)	128 (2)	159 (2)	0.29 (0.02)	0.37 (0.02)
homo $A_{30}B_{30}$	55	324 (40)	308 (39)	341 (42)	0.26 (0.09)	0.3 (0.1)
homo $A_{60}B_{30}$	9	82.9 (0.4)	45.9 (0.5)	100.9 (0.4)	0.135 (0.002)	0.313 (0.006)
homo $A_{60}B_{30}$	18	160 (9)	119 (9)	180 (9)	0.24 (0.03)	0.42 (0.04)
mikto $(A_8B_{15})_2$	5	23.0 (0.1)	19.0 (0.1)	30.3 (0.1)	0.205 (0.003)	0.277 (0.004)
mikto $(A_8B_{15})_2$	15	71.5 (0.9)	66.7 (0.8)	80 (1)	0.312 (0.007)	0.355 (0.007)
mikto $(A_8B_{15})_2$	35	165 (5)	160 (5)	175 (5)	0.29 (0.02)	0.31 (0.02)
mikto $(A_{15}B_{15})_2$	5	31.2 (0.1)	21.9 (0.1)	40.2 (0.1)	0.186 (0.002)	0.312 (0.002)
mikto $(A_{15}B_{15})_2$	10	64.9 (0.6)	54.86 (0.7)	74.9 (0.5)	0.288 (0.007)	0.393 (0.008)
mikto $(A_{30}B_{15})_2$	5	54.2 (0.3)	34.55 (0.3)	63.7 (0.3)	0.195 (0.002)	0.394 (0.003)

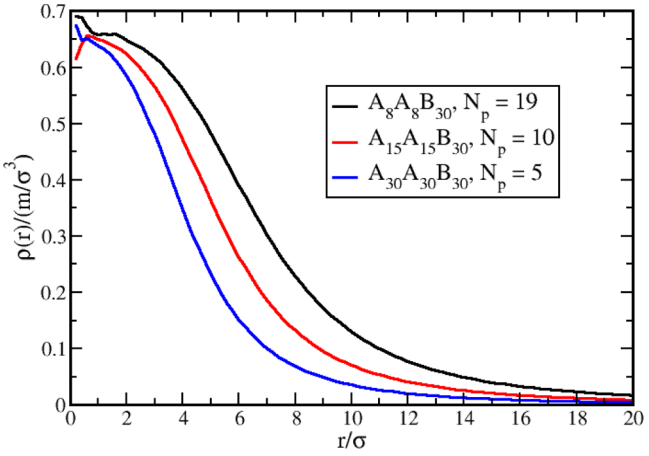

Figure 5. Density profile of aggregates formed by differed Θ-shaped copolymers.

of interest were the critical micelle concentration, the mean aggregation number and the shape of the micelle. We found that for the same solvophilic and solvophobic contents the Θ-shaped copolymers with two solvophobic subchains have higher cmc than the respective Θ-shaped copolymers with one solvophobic subchain. The cmc of mikto figure-eight-shaped copolymers was higher than the respective cmc value of homo figure-eight-shaped, in full agreement with the experimental findings of Isono et al.[9] Similarly, the mikto-linked rings have higher cmc than the homo-linked rings copolymers, and both have higher cmc than the figure-eight-shaped and Θ-shaped copolymers.

Additionally, it is shown that the Θ-shaped copolymers form micelles with preferential aggregation number. The shape of these micelles is spherical with elongated spherical cores. The homo figure-eight-shaped copolymers also form spherical micelles with preferential aggregation number and elongated spherical cores, while the mikto figure-eight-shaped and the linked rings copolymers form wormlike or super structured micelles with wide aggregation numbers. Our results were directly compared with experimental findings of Fan et al.[8] and Isono et al.[9] Further experimental and theoretical studies are required for the elucidation of the role of multiring architecture on the micellization properties of copolymers.

AUTHOR INFORMATION

Corresponding Author

*(C.V.) E-mail: cvlahos@cc.uoi.gr.

Notes

The authors declare no competing financial interest.

ACKNOWLEDGMENTS

We thank Prof. N. Hadjichristidis for suggesting us to study these novel architectures and Kostas Dimakopoulos for technical support. The Research Center for Scientific Simulations (RCSS) of the University of Ioannina is gratefully acknowledged for providing part of the computer resources used in this work.

REFERENCES

(1) Semlyen, J. A. *Cyclic Polymers*; Kluwer Academic Publisher: Dordrecht, The Netherlands, 2000; Chapter 10.

(2) Vlahos, C.; Hadjichristidis, N.; Kosmas, M.; Rubio, A.; Freire, J. Conformational Properties of Ring AB Diblock Copolymers. *Macromolecules* **1995**, *28*, 6854−6859.
(3) Quarti, N.; Viville, P.; Lazzaroni, R.; Minatti, E.; Schappacher, M.; Deffieux, A.; Putaux, J. L.; Borsali, R. Micellar Aggregation in Blends of Linear and Cyclic Poly(styrene-*b*-isoprene) Diblock Copolymers. *Langmuir* **2005**, *21*, 9085−9090.
(4) Marko, J. Microphase Separation of Block Copolymer Rings. *Macromolecules* **1993**, *26*, 1442−1444.
(5) Honda, S.; Yamamoto, T.; Tezuka, Y. Topology-Directed Control on Thermal Stability: Micelles Formed from Linear and Cyclized Amphiphilic Block Copolymers. *J. Am. Chem. Soc.* **2010**, *132*, 10251−10253.
(6) Shi, G.; Pan, C. An Efficient Synthetic Route to Well-Defined Theta-Shaped Copolymers. *J. Polym. Sci., Part A: Polym. Chem.* **2009**, *47*, 2620−2630.
(7) Shi, G.; Yang, L.; Pan, C. Synthesis and Characterization of Well-Defined Polystyrene and Poly(å-caprolactone) Hetero Eight-Shaped Copolymers. *J. Polym. Sci., Part A: Polym. Chem.* **2008**, *46*, 6496−6508.
(8) Fan, X.; Huang, B.; Wang, G.; Huang, J. Synthesis of Amphiphilic Heteroeight-Shaped Polymer Cyclic[Poly(ethylene oxide)-*b*-polystyrene]$_2$ via Click Chemistry. *Macromolecules* **2012**, *45*, 3779−3786.
(9) Isono, T.; Satoh, Y.; Miyachi, K.; Chen, Y.; Sato, S. I.; Tajima, K.; Sato, T.; Kaluchi, T. Synthesis of Linear, Cyclic, Figure-Eight-Shaped, and Tadpole-Shaped Amphiphilic Block Copolymers via *t*-Bu-P$_4$-Catalyzed Ring-Opening Polymerization of Hydrophilic and Hydrophobic Glycidil Ethers. *Macromolecules* **2014**, *47*, 2853−2863.
(10) Kim, S.; Shi, Y.; Kim, J.; Park, K.; Cheng, J. Overcoming the barriers in micellar drug delivery: loading efficiency, in vivo stability, and micelle-cell interaction. *Expert Opin. Drug. Delivery* **2010**, *7*, 49−62.
(11) Nguyen, P. M.; Hammond, P. T. Amphiphilic Linear-Dendritic Triblock Copolymers Composed of Poly(amidoamine) and Poly(propylene oxide) and Their Micellar-Phase and Encapsulation Properties. *Langmuir* **2006**, *22*, 7825−7832.
(12) Cheng, L.; Cao, D. Effect of Tail Architecture on Self-Assembly of Amphiphiles for Polymeric Micelles. *Langmuir* **2009**, *25*, 2749−2756.
(13) Murat, M.; Grest, G. Molecular Dynamics Study of Dendrimer Molecules in Solvents of Varying Quality. *Macromolecules* **1996**, *29*, 1278−1285.
(14) Suek, N.; Lamm, M. Computer Simulation of Architectural and Molecular Weight Effects on the Assembly of Amphiphilic Linear−Dendritic Block Copolymers in Solution. *Langmuir* **2008**, *24*, 3030−3036.
(15) Plimpton, S. Molecular Dynamics Simulator. *J. Comput. Phys.* **1995**, *117*, 1−19.
(16) Georgiadis, C.; Moultos, O.; Gergidis, L. N.; Vlahos, C. Brownian Dynamics Simulations on the Self-Assembly Behavior of AB Hybrid Dendritic−Star Copolymers. *Langmuir* **2011**, *27*, 835−842.
(17) Moultos, O.; Gergidis, L. N.; Vlahos, C. Brownian Dynamics Simulations on Self-Assembly Behavior of H-Shaped Copolymers and Terpolymers. *Macromolecules* **2010**, *43*, 6903−6911.
(18) Moultos, O.; Gergidis, L. N.; Vlahos, C. Self-Assembly Behavior of Thermoresponsive Bis-Solvophilic Linear Block Terpolymers: A Simulation Study. *Macromolecules* **2012**, *45*, 2570−2579.
(19) Tanford, C. *J. Phys. Chem.* **1974**, *78*, 2469−2479.
(20) Nagarajan, R. Molecular theory for mixed micelles. *Langmuir* **1985**, *1*, 331−341.
(21) Tezuka, Y. Topological Polymer Chemistry, Progress of Cyclic Polymers. In *Syntheses, Properties and Functions*; World Scientific Publishing: Singapore, 2013.
(22) Narros, A.; Moreno, A.; Likos, C. Effects of Knots on Ring Polymers in Solvents of Varying Quality. *Macromolecules* **2013**, *46*, 3654−3668.